

Optical links for cryogenic focal plane array readout

Alan R. Johnston
Duncan T. H. Liu, MEMBER SPIE
Siamak Forouhar
George F. Lutes
Joseph Maserjian
Eric R. Fossum, MEMBER SPIE
Jet Propulsion Laboratory
California Institute of Technology
4800 Oak Grove Drive
Pasadena, California 91109
E-mail: duncan@jplpto.jpl.nasa.gov

Abstract. An optical link can provide an interface channel for a focal plane array that is immune to electro-magnetic interference (EMI) and can lower the heat load on the dewar. Our approach involves the use of fiber optics and an on-focal-plane optical modulator to provide an interface to the focal plane array (FPA). The FPA drives the modulator with an electrical signal. We evaluated specially fabricated AlGaAs/GaAs multiple-quantum-well (MQW) optical modulators, operating near 840 nm, for analog modulation, and we have used the results to calculate the performance of an optical interface link using experimentally determined device parameters. Link noise and dynamic range for an analog link were estimated from a separate experiment using pigtailed fiber components. The performance of the MQW modulator system is compared to alternative strategies. Significant improvement in performance in comparison to conventional electronic interfaces appears to be possible.

Subject terms: cryogenic focal plane array; optical fiber link; multiple-quantum-well waveguide modulator.

Optical Engineering 33(6), 2013–2019 (June 1994).

1 Introduction

Optical instruments employing cryogenic focal plane arrays must minimize power dissipation on the focal plane. Because cooler power efficiency is low at cryogenic temperatures, reduction of focal plane power has strong leverage in reducing total system power and cooler mass. Technologies that can reduce total focal plane power dissipation, increase focal plane capability, reduce system power needs, or minimize instrument size and mass are of great interest for maximizing mission lifetime. The cabling between the dewar and the external warm electronics is susceptible to electromagnetic interference (EMI) and thus reduced signal-to-noise (SNR) performance and also provides additional leakage paths for heat to enter the cryogenic system. Reduction in cable channel count can also lead to an increase in system reliability.

Optical interconnects are currently a topic of interest for many electronic and optoelectronic systems.¹ The interconnects can be either free space or guided. The study of guided interconnects (e.g., optical fibers) is driven by the advantages they offer in freedom from EMI and potential bandwidth. Free-space interconnects, although requiring a high degree of mechanical stability and line-of-sight clearances between optical components, offer the possibility of high density interconnects, because optical beams can cross in free space without interaction. The potential for optical interconnects in cryogenic dewar systems has been recognized for several years, but only recently has activity in this area been reported.^{2,3}

In comparison to optical communications applications, where optical data communication speeds exceed 1 Gbit/s, the focal plane application of optical interconnects requires relatively low frequency operation, e.g., from 50 kHz for scientific applications to 100 MHz for some infrared seekers. For the transmission of scientific pixel data, approximately 12 to 14 bits of dynamic range are required. For far-looking infrared (FLIR) and other nonscientific applications, there is a trade-off made for less dynamic range but higher data rate. In a typical scientific system, the electronic multiplexer's output amplifier dissipates approximately 10 mW of power on the focal plane. In higher data rate systems, this can rise to 100 mW dissipated on the focal plane.

In this paper, we explore the use of a fiber optic link between the cryogenic focal plane and the external electronics to replace conventional metallic cabling and electrical interfaces. Our general approach is to locate an optical source, such as a semiconductor laser, outside the dewar in a warm environment where power dissipation is less critical. The light is transmitted to the focal plane where it is modulated, and the optical signal is then transmitted to the warm environment where it can be detected and analyzed. Both digital and analog signals are under consideration. The optical link approach is explored both analytically and experimentally. In particular, an analysis of the system SNR is performed for the optical link in terms of total focal plane power dissipation. Dynamic range is also defined and analyzed. The nonlinearity of the optical link is also discussed. Options and trade-offs such as power dissipation versus speed are considered. Experimental measurements made with an AlGaAs/GaAs multiple-quantum-well (MQW) modulator are reported, and the noise-limited dynamic range of a test link was measured at room temperature.

Paper 21083 received Aug. 26, 1993; revised manuscript received Nov. 13, 1993; accepted for publication Nov. 14, 1993.
© 1994 Society of Photo-Optical Instrumentation Engineers. 0091-3286/94/\$6.00.

2 Optical Link Configuration

The optical readout link configuration we are considering is illustrated in Fig. 1. The figure shows a focal plane array (FPA) and a separate optical waveguide modulator chip mounted in close proximity to it on a common substrate, providing for a minimum length electrical interconnect between the two. The entire assembly is mounted within a dewar at the instrument focal plane. The use of a fiber rather than free-space optics, and a single, rather than multichannel, configuration is essentially an assumption at this point. Alignment of the fiber to the modulator is a critical step, but it can be done under controlled conditions during fabrication. The parts can be cemented into an integral assembly, which maintains alignment thereafter. In addition, the use of fiber optics allows for the readout light to be readily isolated from the FPA by opaque coatings. The FPA itself is assumed to contain circuitry for multiplexing the detector signals into a single serial output and to provide suitable gain to match the output signal levels to the requirements of the modulator. The required signal level can be set between 0.25 and 4 V, by design.

The modulator, seen in Fig. 2, is an AlGaAs/GaAs MQW waveguide device fabricated on a chip 100 to 200 μm long and perhaps 100 μm wide. The use of a modulator of this type for modulation by a low-voltage signal was described by Wiener et al.⁴ Its structure is very similar to that of a laser, with the active waveguide region being a few micrometers deep and less than 10 μm wide. Fiber pigtailed are used as the mechanism for coupling light into and out of the modulator chip, using the techniques commonly used to make a fiber-pigtailed laser. Note that an alternative configuration could be set up with the modulator working in reflection, using the same fiber for both input and output. In this case, a fused coupler outside the dewar would separate the incoming laser beam from the modulated output signal. However, a fundamental problem from increased link noise would have to be dealt with. This possibility is available for future consideration, but will not be discussed here.

A single-mode polarization-preserving fiber must be used between the laser and the modulator because the MQW device is polarization sensitive. A large core, multimode fiber will suffice between the modulator and the receiver outside the dewar. The use of such a fiber would ease the alignment requirements at the output facet of the modulator. The laser and the fiber link design must both be optimized for low noise. The laser wavelength must be carefully matched to the absorption band of the cooled modulator, which will be significantly shifted in wavelength compared to its room temperature value. Actually, it will be desirable to tailor the modulator wavelength to match the laser to take advantage of existing off-the-shelf lasers developed for communication applications. The optical receiver can be a typical low-noise fiber-pigtailed detector-preamp module designed for analog communication applications but modified to optimize its noise over an appropriate band, for example 0 to 1 MHz, for this application.

3 Analysis

3.1 Readout Link Noise and Dynamic Range

In this section, we calculate the theoretical dynamic range of the readout link and relate it to readout bandwidth, modu-

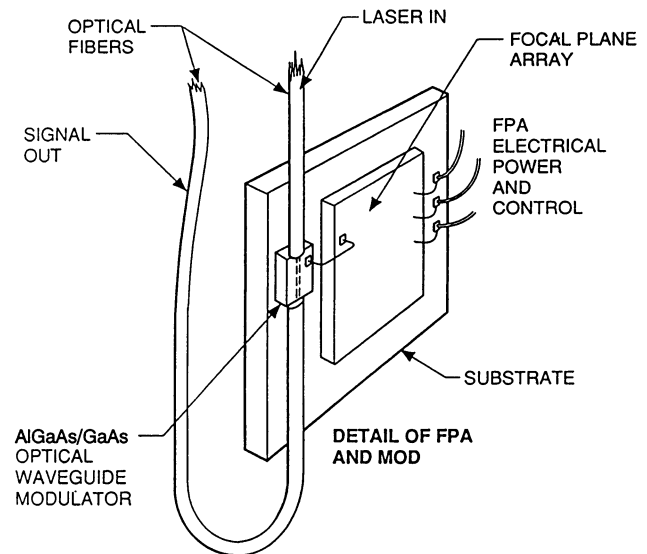


Fig. 1 Sketch illustrating the readout link concept.

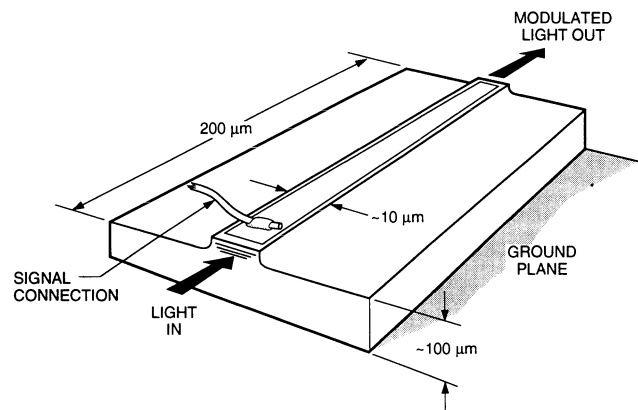


Fig. 2 Sketch of the MQW modulator.

lation index, and optical power. Here P_i is the coupled power from the laser, P_m is the power incident on the modulator, A is an attenuation introduced between laser and modulator, and P_r is the power delivered to the optical receiver. These quantities can be followed through the system using the following expressions:

$$P_m = AP_i \quad (1)$$

$$P_r(t) = LP_m(1 - \beta M) \quad (2)$$

The representation of the modulator, Eq. (2), is arbitrarily set up such that the quantity α is the total insertion loss of the modulator at maximum transmission. The modulation index, $M = [P_r(\text{max}) - P_r(\text{min})]/P_r(\text{max})$, and β ($0 < \beta < 1$) is a time-varying parameter representing the modulator input signal. Note that $P_r(\text{max})$ occurs for $\beta = 0$ and $P_r(\text{min})$ for $\beta = 1$. The quantity $S = P_r(\text{max}) - P_r(\text{min}) = \alpha MP_m$ is the maximum signal swing, also measured at the receiver input.

The rms laser noise δP_q may be related⁵ to the relative intensity noise (RIN) by $\delta P_q^2 = P_i^2 B \cdot \text{RIN}$. The rms quantum noise δP_q is given by

$$\delta P_q = \left(\frac{2h\nu B P_r}{\eta} \right)^{1/2}, \quad (3)$$

where $h\nu$ is the quantum energy (2×10^{-19} at $\lambda = 1 \mu\text{m}$ in mks units), η is the quantum efficiency of the detector, and B is the signal bandwidth, which is defined in our system by the receiver module.

The quantities δP_r , δP_q , and δP_l , which represent the rms value of receiver noise, quantum noise, and laser noise, respectively, are all measured in terms of an equivalent optical noise power [noise-equivalent power (NEP)] at the receiver input. The three principal system noise terms, normalized by the signal swing S , are relative detector noise,

$$\left(\frac{\delta P_r}{S} \right) = \frac{\sqrt{B} \text{NEP}}{M L P_m}, \quad (4)$$

relative quantum noise,

$$\left(\frac{\delta P_q}{S} \right) = \frac{[(1-M)B]^{1/2}}{M} \left(\frac{2h\nu}{\eta L P_m} \right)^{1/2}, \quad (5)$$

and relative laser noise,

$$\left(\frac{\delta P_l}{S} \right) = \left(\frac{1-M}{M} \right) \sqrt{B} \sqrt{\text{RIN}}. \quad (6)$$

The magnitude of each of these terms can be understood as a reciprocal of dynamic range, and they combine in rms fashion to give the total system noise. They are plotted in Fig. 3 for the parameter values given in Table 1 as a function of P_m . It should be kept in mind that the quantum noise given by Eq. (5) represents an optimum theoretical performance. A real optical receiver, especially if required to provide a high dynamic range, will have a somewhat poorer performance. Current in biasing resistors required for the detector to operate properly over the entire dynamic range will add to the noise.⁶ A RIN of -165 dB/Hz, which can be reached with the quietest lasers, will produce a negligible contribution to the total system noise. On the other hand, off-the-shelf multimode diode lasers are much noisier. A RIN = -125 dB/Hz is typical, and would sharply limit link dynamic range.

The total SNR can be scaled to a different system bandwidth by moving all curves vertically by a factor $\sqrt{B/B_0}$, where B_0 is the assumed 1-MHz bandwidth. In the region of operation important for a high-dynamic-range analog link, the quantum noise term [(Eq. (5))] will dominate. The factor $(1-M)^{1/2}/M$ describes its dependence on modulation index. Roughly a factor of 4 improvement in SNR could be obtained by increasing M from 0.5 to 0.9, at the cost of a much larger nonlinearity.

3.2 Electrical Drive Power for the Modulator and Nonlinearity

The preceding analysis did not depend on the details of the modulator, only on the range of its optical transmission. However, nonlinearity and the drive voltage requirement, and with it the electrical drive power, do depend on the transfer function of the modulator. The capacitance of the modulator will be dominated by the interconnection between the FPA and

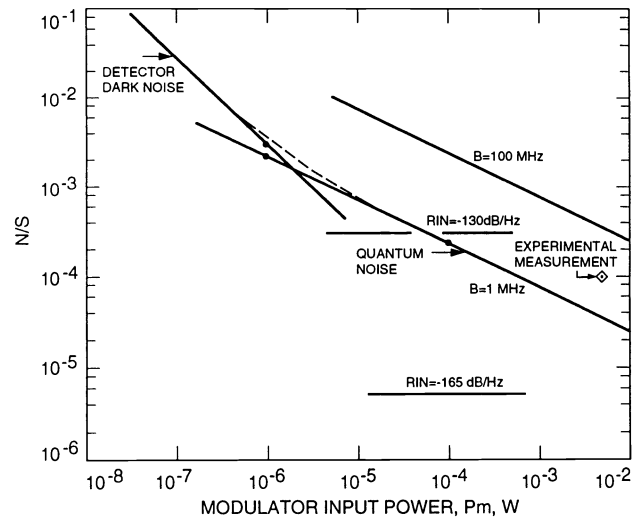


Fig. 3 Link relative noise versus modulator input power.

Table 1 Parameter values used in Fig. 3.

Insertion Loss of Modulator	L	20%
Signal Bandwidth	B	1.0 MHz
Modulation Index	M	0.5
Receiver equivalent input noise	NEP	$-95.0 \text{ dbm/Hz}^{1/2}$

the modulator chip. The electrical power P_e required to drive the modulator is $P_e = 2(1/2 CV^2 f)$. For $f = 1$ MHz, FPA output signal $V = 1$ V, and $C = 1$ pF, P_e becomes $\sim 1 \mu\text{W}$, negligible in comparison to the typical values of P_m , which would be needed to achieve a dynamic range of several thousand.

A crude estimate of nonlinearity can be made by approximating the modulator voltage transfer function by a raised cosine function. For $M = 0.5$, the estimated departure from linearity is $\pm 1/2\%$ from the best fit straight line. The nonlinear term, again very crudely, will vary as M^3 .

4 Experimental Results

4.1 MQW Device Characterization

Figure 4 shows the layer structure of the MQW waveguide modulator that was grown in the Jet Propulsion Laboratory (JPL) Microdevices Laboratory by molecular beam epitaxy (MBE) in a Riber 3200 system. Ohmic contacts were evaporated on the device, and it was then mounted on a laser mount and wire bonded. Current-voltage (I-V) curves were measured with and without incident light, respectively. To induce $1 \mu\text{A}$ of photocurrent, the laser output power had to be increased to about $360 \mu\text{W}$. Therefore, the power dissipation caused by photocurrent will be negligible. In all the absorption and transmission measurements, the optical output power from the waveguide is less than $1 \mu\text{W}$.

A Spectra-Physics Model 3900 Ti:sapphire laser was used to characterize the modulator. Figure 5 shows the relative absorption spectra of the MQW waveguide modulator for different voltages. It shows that the exciton energy without applied voltage is 1.49 eV, which corresponds to $\lambda = 830$ nm. As expected, the exciton energy is shifted to a lower value when the waveguide is reverse biased and to a higher value

Thickness	Material	Dopant Concentration
1000Å	GaAs:Be	1E19
9000Å	GaAs:Be	1.43E18
17600Å	Al _{0.3} Ga _{0.7} As:Si	1E18
870Å	Al _{0.3} Ga _{0.7} As	
90Å	GaAs	
80Å	Al _{0.3} Ga _{0.7} As	
90Å	GaAs	
387Å	Al _{0.3} Ga _{0.7} As	
18100Å	Al _{0.3} Ga _{0.7} As:Si	1E18
3000Å	GaAs:Si	1.43E18

GaAs Substrate

1517Å Field Region 3.72 μm Waveguide Region

Fig. 4 Layer structure of the test MQW waveguide modulator.

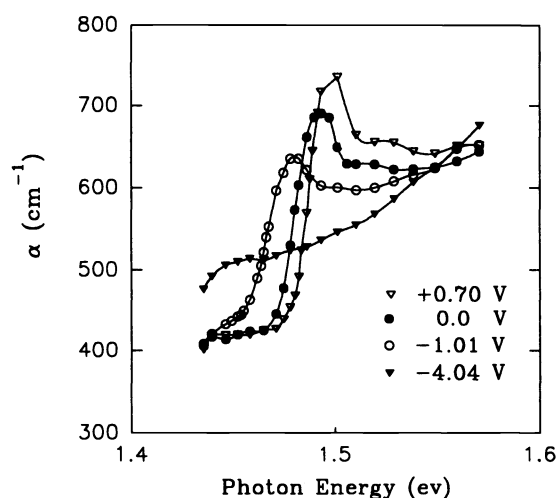


Fig. 5 Absorption spectrum of the test MQW waveguide modulator at various applied voltages.

when the waveguide is forward biased. Furthermore, the exciton peak is broadened as the MQW waveguide is reverse biased. We estimated that the maximum modulation should occur near the tail of the exciton absorption curve at zero applied voltage or about 843 nm. Operating at this wavelength, the signal that drives the modulator will reverse bias the modulator. Because the absorption decreases as the voltage increases, the modulated light is full on when there is no signal.

Figure 6 shows the voltage transfer functions for different wavelengths. In the reverse-biased region, the applied voltage can be as large as 10 V without causing breakdown. In the forward-biased region, the waveguide starts to emit light at 0.85 V. As expected, the largest modulation takes place at $\lambda = 843$ nm. More data points for this wavelength were taken

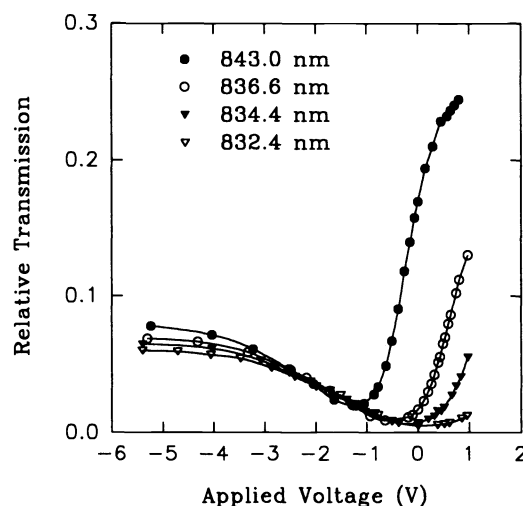


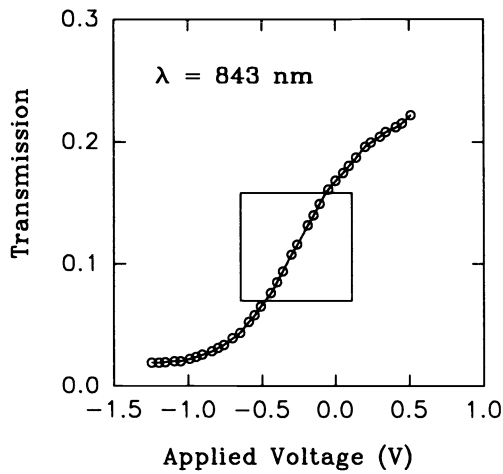
Fig. 6 Relative transmission versus applied voltage of the test MQW modulator at various wavelengths.

and plotted in Fig. 7(a). To check the linearity of the 50% modulation region shown in the box in Fig. 7(a), it is blown up and plotted in Fig. 7(b). The solid line in Fig. 7(b) is the linear least-squares fit of the experimental data. The nonlinearity is estimated to be less than 1% within the 50% modulation limit.

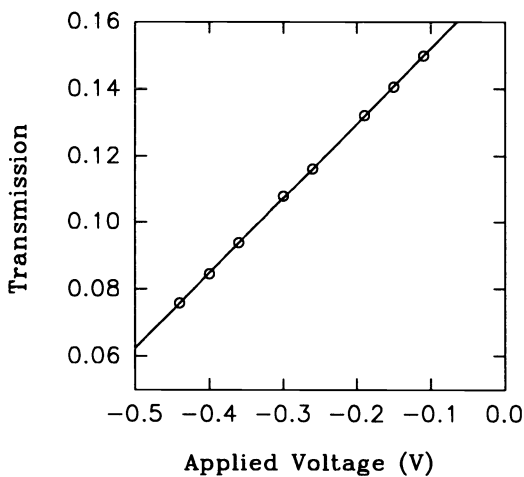
4.2 Link Noise Measurement

An experimental determination of the noise-limited dynamic range of an externally modulated fiber link was made to compare with our theoretical estimate. The fiber optic link was made up of an Ortel 3612B-E01 transmitter, a Crystal Technology MZ 313P lithium niobate waveguide modulator, and an optical receiver assembled in our lab. The noise signal out of the receiver amplifier was applied to a spectrum analyzer and the noise floor was measured over two ranges, 1 to 100 kHz and 1 to 40 MHz. The reading was normalized to 1-Hz bandwidth. The waveguide modulator was replaced with an attenuator for these measurements to avoid the effort necessary to reduce noise peaks from back reflections. The modulator was used to measure the signal swing.

The results of the noise floor measurement for the frequency range from 1 to 100 kHz are shown in Fig. 8. The noise floor curve for the 1- to 40-MHz range was virtually flat, at the -167 dBm/Hz level over the entire frequency range. For both frequency bands, the noise floor signal level is given in terms of an rf power at the output of the optical receiver. It is proportional to the square of the equivalent optical input power to the detector. Note that there is a slight slope to the measured noise versus frequency in the 1- to 100-kHz range, which is consistent with the difference in measured noise levels between the 100-kHz and the 1-MHz points. The peak near zero frequency is a combination of $1/f$ noise and pickup from 60 Hz and its harmonics. The peaks at 26 kHz and 52 kHz are also pickup from local noise sources. These noise peaks are typical in measurements of this type, and are very difficult to eliminate. The -167 dBm/Hz figure is the RIN of the laser transmitter, since the carrier intensity was 1 mW. The measured dynamic range (signal swing \div noise) was 126 dB/Hz at 100 kHz and 137



(a)



(b)

Fig. 7 Modulation transfer function, optical transmission versus applied voltage at $\lambda = 843$ nm: (a) complete curve and (b) magnified plot of the boxed region in (a).

dB/Hz at 1 MHz. Correcting it to be consistent with $B = 1$ MHz and $M = 0.5$, one obtains the data point shown in Fig. 3, which falls above the calculated line by a factor of 3. The agreement seems satisfactory.

5 Discussion and Conclusions

Our results indicate that readout of an FPA using fiber optics is feasible at room temperature and may achieve a significant reduction in the heat load on the focal plane. In addition, crosstalk in the readout link itself will be reduced, and heat conduction by the readout cabling will also be decreased. The calculated link performance indicates that for a representative FPA requirement (1 to 2 MHz signal bandwidth), the heat load in the Dewar resulting from the readout link could be a few tenths of a milliwatt, assuming a dynamic range of 5000. This compares to approximately 60-mW dissipation measured for a conventional electronic output amplifier providing similar performance. The bandwidth of the readout link is not limited by any characteristic of the link;

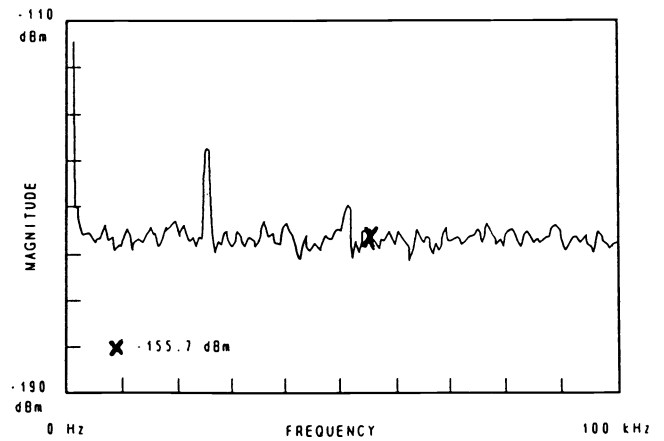


Fig. 8 Measured noise versus frequency spectrum of link output from 0 to 100 kHz.

analog fiber optic data transmission is being actively pushed into the microwave region.⁷⁻⁹ However, the inherent power speed trade-off would require increased power dissipation on the focal plane at a higher data rate. For example, to provide a 100-MHz signal bandwidth, the link dissipation would become several tens of megawatts to maintain the assumed dynamic range of 5000. This cryogenic heat load is dominated by the optical power input to the modulator because most of it is dissipated in the modulating element. The electrical power required to drive the modulator is negligible. Thus, the most effective step toward improving the link power dissipation would be to lower the insertion loss of the modulator. The best achievable value of insertion loss is probably near 3 to 4 dB, limited by the coupling from the cylindrical fiber core to the planar modulator waveguide. We have assumed 7 dB in our analysis.

Dynamic range in the operating regime of interest is limited by quantum noise (equivalent to shot noise in the photocurrent) in the optical signal. Detector noise, for a well-designed receiver module, will be swamped out by the relatively high optical signal level. In general, dynamic range can be increased by increasing the power incident on the modulator, so an inherent tradeoff results between dynamic range and heat load. The effect of laser noise (RIN noise) for a diode laser source can be made negligible if optimum techniques are used. However, note that it is extremely important to minimize or eliminate all back reflections that could return part of the optical signal to the laser. Diode lasers are very sensitive to back reflection and their RIN can easily be increased by 40 dB (two orders of magnitude in terms of optical noise power) if back reflections are significant. In such a case, the system dynamic range will be limited by laser noise, and further improvement of dynamic range by increasing the link power is no longer possible. Angle polished connectors, nonreflecting attenuators, optical isolators, and optimum antireflection treatment of the modulator to fiber coupling should all be incorporated.¹⁰

There are alternative configurations for an optical readout link that we have considered briefly in this work. The alternatives involve three areas: the type of optical modulator; the use of parallelism in the readout, which is often cited as an inherent strong point for optics; and the possibility of digital readout.

Waveguide modulators of the Mach-Zender or delta-beta types could be used in place of the MQW modulator we investigated. An advantage of this type of modulator is a potential decrease in optical insertion loss. They are phase modulators with no absorption being involved in the modulation process. MQW modulators can be configured to work in a phase mode, and there are indications that a very strong phase effect can be realized in MQW structures.¹¹ Alternatively, phase modulators using either LiNbO₃ (Refs. 12 and 13; also see, for example, waveguide modulator Model 4531 made by United Technologies Photonics, New Focus, Mountain View, California) or nonlinear polymers^{14,15} could be used. There are no known materials limitations that would preclude using either of these at cryogenic temperatures. As a practical matter, the difficulty of coupling a fiber to a planar waveguide is a similar limitation in all these modulator types. Further, the modulating voltage requirement of either LiNbO₃ or NL polymer modulators appears to be somewhat larger, and their physical size is very much larger than the MQW type. On balance, it seems that the MQW modulator is the best choice due to dewar coldfinger size constraints.

A brief look at the possible advantages of a highly parallel (and therefore lower bandwidth) readout structure is inconclusive at this point. For example, a scaling analysis showed that multiple fiber links, one for each row (or pixel) do not use significantly less power in total. Free-space optics could be used to eliminate the need for a large number of fibers in a highly parallel readout arrangement. However, the use of free-space optics would greatly complicate the design of the focal plane configuration to rigorously separate the readout light from the low-level image light and also to maintain alignment between the optical components inside and those outside of the dewar.

The scaling analysis did indicate that a different type of parallelism, namely one where the dynamic range of the output signal is subdivided (of which digital encoding is one example) can result in a significant power saving. For a digital readout link, the conclusion seems quite clear cut; it performs much better than an equivalent analog one. A digital link is essentially an ideal channel, both in terms of fidelity and power, in comparison to other elements of the system. However, the challenge has simply been transferred to an analog-to-digital (A/D) circuit, which must now be incorporated in the focal plane. It is not yet clear whether an overall net improvement in performance can be achieved, but related topics are being actively pursued.¹⁶⁻¹⁸

Several things remain to be done before successful hardware can be implemented. The most important issue is to determine what effects the cryogenic environment will have on the parts of the readout link that will be located in the dewar. Changes in modulator parameters can be expected, as well as mechanical effects from differential expansivity. The working optical wavelength of the modulator will decrease, and its transfer function should become steeper. There is no performance penalty expected from the wavelength shift, but it is a large shift, expected to be about 50 nm, and must be allowed for in design. The change to be expected in the slope of the modulation curve is not known at this point, but it should be small. Equally important, the effect of thermal strains associated with the mounting of the modulator chip and the fiber pigtails can be critical. Development of practical fabrication techniques that will withstand the thermal cycling

without causing an unacceptable impact on performance is vital. The insertion loss at maximum transmission is a very important parameter. Optimization of the fiber-to-modulator-chip coupling is needed, and is closely related to the mechanical thermal design issue. Finally, for an optical readout link to function properly in a system sense, suitable electronic stabilization techniques must be developed to maintain the desired operating conditions and with them the calibration of the readout process.

Acknowledgments

We would particularly like to thank Anders Larsson, now at Chalmers University, Goteborg, Sweden, who was involved in early discussions of the idea, before the present task began. The MBE work to produce the wafers from which our test devices were made was carried out by John Liu and Robert Conley in JPL's Microdevices Laboratory. The test devices were prepared by Sam Keo, also in the Microdevices Laboratory. Finally, we thank Thomas Wood of ATT Bell Laboratories for helpful discussions of the modulating devices, and Frank Jaworski of Loral, Inc., Lexington, Mass., who provided insights into current system applications. The work described in this paper was supported by the JPL Director's Discretionary Fund. It was carried out as part of the Center for Space Microelectronics Technology Program at the Jet Propulsion Laboratory, California Institute of Technology, and was sponsored by the National Aeronautics and Space Administration (NASA). Reference herein to any specific commercial product, process, or service does not imply its endorsement by the United States Government, NASA, or the Jet Propulsion Laboratory.

References

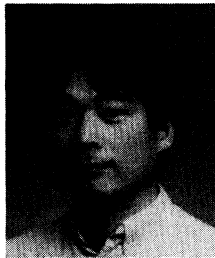
1. See, for example, *Optoelectronic Materials, Devices, Packaging and Interconnects*, T. E. Batchman, R. S. Carson, R. L. Gallawa, and H. J. Wojtunik, Eds., *Proc. SPIE* **836** (1987); *Optoelectronic Materials, Devices, Packaging and Interconnects II*, G. M. McWright and H. J. Wojtunik, Eds., *Proc. SPIE* **994** (1988).
2. E. R. Fossum, "Photonic interconnections: more bandwidth, less real estate," *Photon. Spectra* **21**, 151-157 (1987).
3. E. R. Fossum, A. G. Larsson, and J. Maserjean, "Optical link for readout from a focal plane array," *NASA Tech. Brief* **16**, 30-31 (1992).
4. J. S. Weiner, A. C. Gossard, J. H. English, D. A. B. Miller, D. C. Chemla, and C. A. Burrus, "Low-voltage modulator and self-biased self electro-optic device," *Electron. Lett.* **23**, 75-77 (1987).
5. G. P. Agrawal and N. K. Dutta, *Long-wavelength Semiconductor Lasers*, pp. 247-252, Van Nostrand Reinhold, New York (1986).
6. T. V. Muoi, "Receiver design for high speed fiber optic systems," *J. Lightwave Technol.* **2**, 243-267 (1984).
7. W. E. Stephens and T. R. Joseph, "System characteristics of direct modulated and externally modulated RF fiber-optic links," *J. Lightwave Technol.* **5**, 380-387 (1987).
8. G. E. Betts, L. M. Johnson, and C. H. Cox, III, "High dynamic range, low-noise analog optical links using external modulators: analysis and demonstration," *Proc. SPIE* **1371**, 252-257 (1990).
9. G. E. Betts, L. M. Johnson, and C. H. Cox, III, "Optimization of externally modulated analog optical links," *Proc. SPIE* **1562**, 281-302 (1991).
10. R. T. Logan and G. F. Lutes, "High stability microwave fiber optic systems: demonstrations and applications," in *Proc. 46th Ann. Symp. on Frequency Control*, IEEE, Ultrasonics, Ferroelectrics, and Frequency Control Society, and Army Research Lab., pp. 310-316, Hershey, PA (1992); R. T. Logan, G. F. Lutes, L. E. Primas, and L. Maleki, "Design of a fiber optic transmitter for microwave analog transmission with high phase stability," in *Dept. of Defense Fiber Optics Conference '90*, pp. 359-365 (1990).
11. C. Thirstrup, "Novel electro-optical phase modulator based on GaInAs/InP modulation doped quantum-well structures," *Appl. Phys. Lett.* **61**, 2641-2643 (1992).
12. H. Kogelnik and R. V. Schmitt, "Switched directional couplers with alternating $\Delta\beta$," *IEEE J. Quantum Electron.* **12**, 396-401 (1976).

13. R. C. Alfrnss, "Waveguide electrooptic modulator," *IEEE Trans. Microwave Theory Tech.* **30**, 1121–1137 (1982).
14. E. Van Tomme, P. P. Van Daele, R. G. Baets, and P. E. Lagasse, "Integrated optic devices based on nonlinear optical polymers," *IEEE J. Quantum Electron.* **27**, 778–786 (1991).
15. E. Van Tomme, P. P. Van Daele, R. G. Baets, G. R. Mohlmann, and M. B. J. Diemeer, "Guided wave modulators and switches fabricated in electro-optic polymers," *J. Appl. Phys.* **69**, 6273–6276 (1991).
16. Tushar R. Gheewala, "Josephson-logic devices and circuits," *IEEE Trans. Electron. Devices* **27**, 1857–1869 (1980).
17. K. K. Likharev and V. K. Semenov, "RFSQ logic/memory family: a new Josephson junction technology for sub terahertz clock frequency digital systems," *IEEE Trans. Appl. Superconductivity* **1**, 3–28 (1991).
18. E. A. Vittoz, "The design of high-performance analog circuits on digital CMOS chips," *IEEE J. Solid State Circuits* **20**, 657–665 (1985).



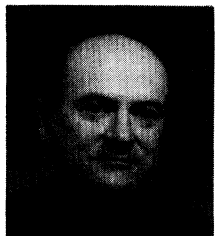
Alan R. Johnston received the BS in physics in 1952 and the PhD in physics in 1956, both from the California Institute of Technology. Aside from a brief period as a visiting professor at Chalmers Technical University in Goteborg, Sweden, Dr. Johnston has been at the Jet Propulsion Laboratory (JPL), California Institute of Technology, since 1956. He has conducted research on inertial guidance systems, electro- and ferro-optic materials, and

proximity sensing devices for robotics. In 1974, he initiated a fiber optics R&D program at JPL aimed at NASA applications. From 1982 to 1989, he built up and supervised an optical information processing research group. Dr. Johnston's current research interests are fiber sensing, optical computing, and fiber networking, as well as optical interconnection techniques. His fiber optics R&D activities currently include the investigation of space environmental effects on fiber optics related to an orbital fiber optics experiment launched in April 1984. Dr. Johnston is a member of the Optical Society of America and Sigma Xi.



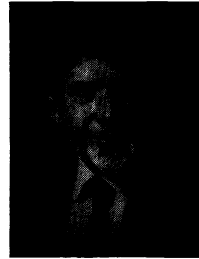
Duncan T. H. Liu received his BS in physics from National Cheng-Kung University, Taiwan, in 1978; his MS in physics from Wayne State University in 1984; and his PhD in electrical engineering from Pennsylvania State University in 1987. His PhD research work was on nonlinear optical properties of liquid crystals. Since 1987, he has been a member of the technical staff at Jet Propulsion Laboratory, where he has conducted research on photorefractive devices, optical image processing, adaptive optics, wavelength division multiplexing, and radiation effects in fibers. His current research interests include fiber linked and powered sensor networks, holographic optical storage devices, and electro-optic systems in general. Dr. Liu has authored and coauthored 20 papers and received two patents. He is a member of SPIE, IEEE, and OSA.

Siamak Forouhar: Biography and photograph not available.



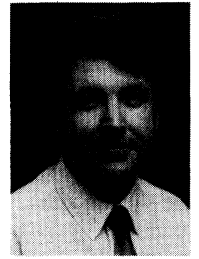
George F. Lutes attended various colleges including West Coast University prior to and during most of his career working in the aerospace industry. He began his career in 1959 working on radar systems at North American Aircraft Autonetics Division. From 1962 to 1964, he worked at TRW where he developed high-frequency transistorized circuitry for use on satellite systems. Since 1964, he has been employed at the Jet Propulsion Laboratory

(JPL). He worked on atomic frequency standard development at JPL until 1978. In 1978 he became interested in fiber optics and photonics and has concentrated on developments in that technology since that time. He has authored or coauthored more than 40 papers and has six patents in the areas of high stability, low phase noise, RF electronic circuits, and high stability, low phase noise, RF and microwave fiber optic and photonic systems. His main interests are high performance analog fiber optic microwave transmission systems and analog photonic microwave signal processing systems. He is currently working on fiber optic antenna remoting systems and photonic microwave signal processing for the NASA Deep Space Network.



Joseph Maserjian received his BS in physics from Rensselaer Polytechnic Institute in 1952, his MS in physics from the University of Southern California in 1955, and his PhD in materials science from California Institute of Technology in 1966. From June 1952 to 1960, he was on the technical staff at Hughes Semiconductors. Since January 1960, he has been with the Jet Propulsion Laboratory where he is a senior research scientist and currently

holds the position of division technologist. His work has included semiconductor materials and devices, insulating films, tunneling, and very large scale integration reliability physics. In 1985, he received the NASA Medal for Exceptional Scientific Achievement. He has filed more than 30 patents and has published more than 90 technical papers. His recent research interest is MBE-engineered semiconductor devices, including infrared detectors, optical modulators, and submillimeter-wave oscillators and multipliers.



Eric R. Fossum received his BS degree with honors in physics and engineering from Trinity College, Connecticut, in 1979, his MS degree in 1980 from Yale University in applied physics, and his PhD from Yale in electrical engineering in 1984. Dr. Fossum has held an IBM Graduate Fellowship and the Howard Hughes Doctoral Fellowship. He joined Columbia University in 1984 as an assistant professor, and was engaged in research on silicon charged-

coupled devices (CCDs) for on-focal-plane image processing and III-V CCDs for very high speed signal processing. His other activities included novel devices and structures for fiber-based optical interconnects and the low-energy ion-beam modification of semiconductor surfaces. Dr. Fossum was promoted to associate professor in 1989. He joined the Jet Propulsion Laboratory (JPL) in 1990 and manages the research and advanced development of image sensors and infrared focal plane technology. He continues his own research in active pixel image sensors, on-chip signal processing, and III-V devices. Dr. Fossum has received several awards including the Yale Becton Prize in 1984, the IBM Faculty Development Award in 1984, the National Science Foundation Presidential Young Investigator Award from President Reagan in 1986, and the JPL Lew Allen Award for Excellence in 1992. He has organized several conferences including the 1986 IEEE Workshop on CCDs, the 1990 IEEE Workshop on Advanced Solid-State Image Sensors, and the 1992 SPIE Conference on Infrared Readout Electronics. He also cochaired the 1991 IEEE Workshop on CCDs and the 1993 IEEE Workshop on CCDs and Advanced Image Sensors. Dr. Fossum has published over 100 technical papers, served on several IEEE and SPIE conference committees, and is a senior member of the IEEE and a member of the APS and SPIE.